Carbohydrate Polymers 103 (2014) 119–125

Contents lists available at ScienceDirect

Carbohydrate Polymers

journal homepage: www.elsevier.com/locate/carbpol

# Isolation and characterization of cellulose nanowhiskers from oil palm biomass microcrystalline cellulose

M.K. Mohamad Haafiz[a,b], Azman Hassan[a,*], Zainoha Zakaria[c], I.M. Inuwa[a]

[a] Department of Polymer Engineering, Faculty of Chemical Engineering, Universiti Teknologi Malaysia, UTM 81310, Skudai, Johor, Malaysia
[b] School of Industrial Technology, Universiti Sains Malaysia, 11800 Penang, Malaysia
[c] Department of Chemistry, Faculty of Science, Universiti Teknologi Malaysia, UTM 81310, Skudai, Johor, Malaysia

ARTICLE INFO

*Article history:*
Received 4 October 2013
Received in revised form
14 November 2013
Accepted 27 November 2013
Available online 6 December 2013

*Keywords:*
Microcrystalline cellulose
Cellulose nanowhiskers
Transmission electron microscopy
Oil palm biomass

ABSTRACT

The objective of this study is to compare the effect of two different isolation techniques on the physicochemical and thermal properties of cellulose nanowhiskers (CNW) from oil palm biomass obtained microcrystalline cellulose (MCC). Fourier transform infrared analysis showed that there are no significant changes in the peak positions, suggesting that the treatments did not affect the chemical structure of the cellulose fragment. Scanning electron microscopy showed that the aggregated structure of MCC is broken down after treatment. Transmission electron microscopy revealed that the produced CNW displayed a nanoscale structure. X-ray diffraction analysis indicated that chemical swelling improves the crystallinity of MCC while maintaining the cellulose I structure. Acid hydrolysis however reduced the crystallinity of MCC and displayed the coexistence of cellulose I and II allomorphs. The produced CNW is shown to have a good thermal stability and hence is suitable for a range of applications such as green biodegradable nanocomposites reinforced with CNW.



## 1. Introduction

In recent years, there is a growing interest in the development of biodegradable products using innovative processing technologies from renewable resources that offer sustainability and reduced dependence on fossil fuel (Cherian et al., 2011; Deepa et al., 2011). In this context, a renewable biopolymer resource that has high potential as a raw material for sustainable production is cellulose which occurs in abundance in nature, relatively cheap and biodegradable (Deepa et al., 2011; D. Liu, Zhong, Chang, Li, & Wu, 2010). Cellulose is a linear homopolymer of glucose $(C_6H_{10}O_5)n$ linked by 1, 4-β-glycosidic bonds with cellobiose, a dimer, as its repeating unit which is bound together by lignin and hemicelluloses (Filson & Dawson-Andoh, 2009; Li et al., 2009).

In nature, cellulose molecular chains are biosynthesized, self-assembled and repeatedly aggregated along cellulose chains to form microfibrils, which are composed of crystalline and amorphous domains (Eichhorn, 2010; Fernandes et al., 2011; Nishiyama, 2009). Cellulose I only exists in two allomorphs which are the crystalline structure in nature (Filson & Dawson-Andoh, 2009). The fiber bundles of cellulose molecules are stabilized laterally by hydrogen bond between hydroxyl groups (Nishiyama, 2009). Cellulose fibers obtained from different sources or their derivatives have been used in a different type of products for a long time. However, it has only been known that acid hydrolysis of cellulose fibers yielded very crystalline rodlike cellulose nanocrystals (CNC), also called cellulose nanowhiskers (CNW) or nanocrystalline cellulose (NCC) or even monocrystal despite their nanoscale dimension (Bras et al., 2010; Brito, Pereira, Putaux, & Jean, 2012).

CNW has gained considerable interest because of their unique and attractive features i.e. cost effectiveness, high aspect ratio, and light weight (H. Liu, Liu, Yao, & Wu, 2010). Indeed the tensile strength of whiskers is far above those of current high-volume content reinforcements, allowing the processing of the highest attainable composite strengths (Bondeson, Mathew, & Oksman, 2006; D. Liu et al., 2010). They are also ideal as reinforcement's materials in a transparent polymeric matrix because they do not cause light scattering. This is due to their lateral dimensions smaller than the wavelength of visible light e.g. bacterial cellulose fibrils (Yano et al., 2005).

CNW can be prepared by acid hydrolysis of any natural source of cellulose. The controlled acid hydrolysis readily degrades the amorphous regions of the cellulose microfibrils, leaving the crystalline segments intact and leading to the formation of single crystals (Rånby, 1951; Samir, Alloin, & Dufresne, 2005). The length and

* Corresponding author at: Department of Polymer Engineering, Faculty of Chemical Engineering, Universiti Teknologi Malaysia, 81300 Skudai UTM, Johor, Malaysia. Tel.: +60 7 5537835; fax: +60 7 5581 463.
*E-mail addresses:* azmanh@cheme.utm.my, azmanpolymer@gmail.com (A. Hassan).

0144-8617/$ – see front matter © 2013 Elsevier Ltd. All rights reserved.
http://dx.doi.org/10.1016/j.carbpol.2013.11.055

width of the CNW mainly depend on the cellulose source and the acid hydrolysis conditions (Brito et al., 2012). It is difficult to obtain uniformly dispersed CNW from natural plant fibers because the nano-phase has a strong tendency to form larger structures via aggregation and agglomeration (D. Liu et al., 2010). However, when subjected to mechanical dispersion or ultrasonification, it permits the dispersion of CNW aggregates, resulting in the production of stable colloidal suspensions (Filson & Dawson-Andoh, 2009; Pandey, Chu, Kim, Lee, & Ahn, 2009). As reported earlier (Filson & Dawson-Andoh, 2009; Petersson, Kvien, & Oksman, 2007), proper treatment of microcrystalline cellulose (MCC) with sulfuric acid ($H_2SO_4$) provides not only isolated cellulose whiskers but also yields a negatively charged surface resulting from the esterification of hydroxyl groups by sulphate ions forming a stable colloidal dispersion. Another alternative way to produce CNW from MCC is chemical swelling and ultrasonic treatment method proposed by Oksman, Mathew, Bondeson, and Kvien (2006).

The present paper describe, for the first time to our knowledge, the isolation and detailed characterization of CNW from MCC obtained from completely chlorine free oil palm empty fruit bunch (OPEFB) pulp. The isolation and characterization of MCC from OPEFB has previously been reported by the present authors (Haafiz, Eichhorn, Hassan, & Jawaid, 2013). OPEFB is the fibrous mass left behind after separating the fruits from sterilized fresh fruit bunches (Shinoj, Visvanathan, Panigrahi, & Kochubabu, 2011). This highly cellulosic material is presently used as fuel, fertilizers or mulching material (Hassan, Salema, Ani, & Bakar, 2010). OPEFB fibers are already recognized as a natural reinforcing component but their use as a viable bioresource to produce CNW has not received attention yet, despite increasing efforts to find high-added value application for this fiber. In addition, CNW characterization was compared by using two different isolation techniques, acid hydrolysis and chemical swelling treatment. The aim of this comparison was to address the question of the influence of the different isolation technique on the properties of the CNW obtained.

## 2. Experimental

### 2.1. Materials

Microcrystalline cellulose (MCC) was produced from oil palm empty fruit bunch (OPEFB) chlorine free pulps. The production of MCC was described in detail in our previous paper (Haafiz et al., 2013). All chemicals were used as received and were secured from Merck, Malaysia.

### 2.2. Preparation of CNW

#### 2.2.1. Acid hydrolysis

Colloidal suspension of CNW in water was prepared as described in detail elsewhere (Bondeson et al., 2006; Li et al., 2009). For 5 g of MCC were hydrolyzed in 64% $H_2SO_4$ (96% purity) solution with an acid to MCC ratio of 8.75 ml/g at 40 °C for 60 min with strong agitation. The on-going hydrolysis was stopped by adding 4–5 times cold distilled water based on the volume of the reacting mixture. The diluted suspension was centrifuged using Universal 32 Hettich (Newport Pagnell, England) at 5000 rpm for 15 min to get the precipitates. The precipitate was suspended in distilled water, followed by centrifugation. This process was repeated until the supernatant solution became turbid and further the colloidal suspension was collected and sonicated for 30 min. Sonication was done in cold water bath to avoid heat-up. Subsequently, the suspension was stored in a refrigerator at 4 °C and designated CNW.

#### 2.2.2. Chemical swelling

MCC was swelled and partly separated to whiskers by chemical and ultrasonification treatments using the same method as described by Pereda, Amica, Rácz, and Marcovich (2011) based on original procedures described by Oksman et al. (2006). *N*,*N*-Dimethylacetamide (DMAc) (99% purity) with 0.5% lithium chloride (LiCl) (99% purity) solution was used as swelling agent. The initial concentration of MCC in DMAc/LiCl was 10 wt%. The MCC was agitated using a mechanical stirrer inside a water bath for 12 h at 70 °C. The slightly swelled particles were then sonicated in a Branson 2510 bransonic bath for 3 h over a period of 5 days, with long intervals between each sonication treatment to separate the cellulose nanowhiskers. The resultant cellulose nanowhiskers were repeatedly washed with distilled water then freeze-dried and noted as CNW/S.

## 3. Characterization

### 3.1. Fourier transform infrared spectroscopy

Fourier transform infrared spectroscopy (FT-IR) was measured by direct transmittance by means of the KBr pellet technique using a Perkin Elmer 1600 infrared spectrometer (Nicolet AVATAR 360) at 32 scans with a resolution of 4 $cm^{-1}$ and within the wave number range of 370–4000 $cm^{-1}$. The position of significant transmittance peaks was determined using the "find peak tool" provided by Nicolet OMNIC 5.01 software.

### 3.2. Microscopic analysis

#### 3.2.1. Scanning electron microscopy

Scanning electron microscopy (SEM) was carried out using a SEM-EDX Oxford INCA 400 model at an acceleration voltage of 15 kV. The samples were sputter-coated with gold to avoid charging.

#### 3.2.2. Transmission electron microscopy

The dimensions of the prepared samples were obtained from transmission electron microscopy (TEM) model LEOLIBRA at an accelerating voltage of 120,000. The 5 μL suspension samples were placed on a carbon-coated grid and allowed to dry at room temperature. The TEM images were obtained using soft imagine system software.

### 3.3. X-ray diffraction

X-ray diffraction (XRD) was carried out to study the crystallinity of the samples using an X'Pert X-ray diffractometer (SIEMENS XRD D5000) and Ni-filtered Cu Kα radiation at an angular incidence of 10–60° (2$\theta$ angle range). The operating voltage and current were 40 kV and 50 mA, respectively. The crystallinity of the samples was calculated from diffraction intensity data using the empirical method for native cellulose (Rosa, Rehman, De Miranda, Nachtigall, & Bica, 2012; Tang et al., 2013). The crystalline-to-amorphous ratio of materials was determined using Eq. (1).

$$C_rI \quad (\%) = \frac{I_{002} - I_{am}}{I_{002}} \tag{1}$$

where $C_rI$ is the crystallinity index, $I_{002}$ is the maximum intensity (in arbitrary units) of the diffraction from the 0 0 2 plane at $2\theta = 22.6°$, and $I_{am}$ is the intensity of the background scatter measured at $2\theta = 19°$.

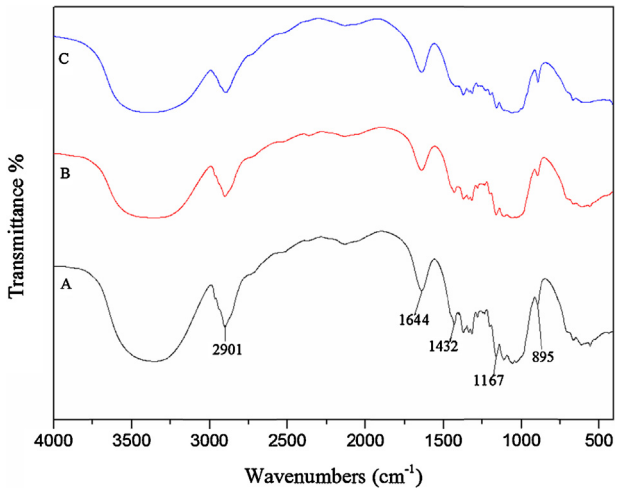


**Fig. 1.** Typical FT-IR spectroscopy for (A) MCC, (B) CNW/S and (C) CNW.

### 3.4. Thermogravimetric analysis

The thermal stability of samples was characterized using a thermogravimetric analyzer, model 2050 (TA Instruments, New Castle, DE). The specimens were scanned from 30 °C to 900 °C at a rate of 10 °C min$^{-1}$ under a nitrogen gas atmosphere.

## 4. Results and discussion

### 4.1. FT-IR spectroscopic analysis

The investigation into changes in chemical structure of MCC after chemical swelling and acid hydrolysis treatment was carried out through FT-IR absorption spectroscopy. FT-IR spectroscopy is an indispensable technique and a relatively easy method to obtain direct information on any changes in the chemical structure of cellulose after chemical treatment (Jonoobi, Khazaeian, Md.Tahir, Azry, & Oksman, 2011; Mandal & Chakrabarty, 2011). Typical FT-IR spectra of MCC, CNW/S and CNW are illustrated in Fig. 1(A)–(C). The vibrational assignments are summarized in Table 1. FT-IR spectroscopy revealed the similarities of all spectra which is an indication that all samples have similar chemical composition. Similar results were obtained by Fahma, Iwamoto, Hori, Iwata, and Takemura (2010) when isolating nanofibres from OPEFB using different concentrations of sulfuric acid ($H_2SO_4$).

The absorption around 3400, 2900, 1430, 1370, 890 cm$^{-1}$ exhibited in all spectra is associated with the characteristics of native cellulose I (Tang et al., 2013). The broad absorption band located between 3400 and 3500 cm$^{-1}$ is due to stretching of —OH groups and an absorption at 2900 cm$^{-1}$ is related to $CH_2$ groups of cellulose (Jain & Vigneshwaran, 2012; Jonoobi et al., 2011; Rosa et al., 2012). In addition, the appearance of a peak at around 1645 cm$^{-1}$ in all samples is indicative of absorption of water by cellulose. According to other studies, this band is related to the bending modes of water molecules due to a strong interaction between cellulose and water (Johar, Ahmad, & Dufresne, 2012; Jonoobi et al., 2011; Rosa et al., 2012). Additionally the absorption band at 1428–1433 cm$^{-1}$ is associated with intermolecular hydrogen attraction at the $C_6$ group (Kumar, Maria De La, & Yang, 2002).

Meanwhile the peak appearing in the 1330–1369 cm$^{-1}$ range in the spectra of all samples is attributed to the bending vibration of the C—H and C—O groups of aromatic ring in polysaccharides. Similar results are also presented in a report by Jonoobi et al. (2011) in the study of nanofibers from OPEFB by chemo-mechanical process and by Mandal and Chakrabarty (2011) in isolating nanocellulose from waste sugarcane bagasse. The ring breathing band at 1163–1167 cm$^{-1}$ corresponds to C—C and the C—O—C glycosidic ether band was at 1105 cm$^{-1}$. The latter peak is gradually lost in CNW due to hydrolysis treatment and concomitant reduction in molecular weight (Mandal & Chakrabarty, 2011). The peak at 894–896 cm$^{-1}$ is associated with C—H rocking vibration of cellulose (anomeric vibration, specific for β-glucosides) observed in MCC, CNW/S, and CNW samples (Fahma et al., 2010; Li et al., 2009).

The FT-IR spectra show that the chemical swelling and acid hydrolysis reaction performed to obtain CNW/S and CNW from MCC does not affect the chemical structure of the cellulosic fragments. This indicates that the chemical groups of the resulting materials were stable and no strong chemical reaction occurred (Chen, Liu, Chang, Cao, & Anderson, 2009). However, their surface morphologies may be affected.

**Table 1**
FT-IR spectral peak assignments for MCC, CNW/S, and CNW.

| Peak frequency (cm$^{-1}$) for MCC, CNW/S and CNW | | | |
|---|---|---|---|
| Peak assignment | MCC | CNW-S | CNW |
| OH groups | 3471 | 3483 | 3493 |
| $CH_2$ groups | 2901 | 2902 | 2902 |
| C=O stretching | 1644 | 1641 | 1644 |
| $CH_2$ bending | 1432 | 1428 | 1433 |
| C—H asymmetric stretching | 1374 | 1376 | 1377 |
| C—O—C stretching | 1167 | 1163 | 1167 |
| C—H | 895 | 896 | 894 |

### 4.2. Scanning electron microscopy

The morphology of MCC after chemical swelling and acid hydrolysis treatment was explored by means of SEM at the micron and submicron level. It is worth noting, however, as seen in Fig. 2(B), that chemical swelling and acid hydrolysis (Fig. 2(C)) altered the morphology of the MCC. Untreated MCC (Fig. 2(A)) display aggregated irregular shaped fibrils, and a rough surface morphology, with presumably lower aspect ratios. It is reported that these aggregated MCC are composed of strong hydrogen bonding between hundreds of individual cellulose whiskers (D. Liu et al., 2010; Mathew, Oksman, & Sain, 2005; Petersson et al., 2007). In addition, according to an earlier study by Mathew, Oksman, and Sain (2006), the roughness of MCC favors the production of nanocrystals via hydrolysis. Likewise the MCC obtained from different sources and hydrolysis conditions differ in overall characteristics such as particle size and aggregation (De Menezes, Siqueira, Curvelo, & Dufresne, 2009; Lee et al., 2009).

It is clear from typical SEM micrographs in Fig. 2(B) and (C) that the aggregation of MCC was broken down after chemical swelling and acid hydrolysis. The tendency of fiber separation can clearly be observed after both treatments gave rise to intermittent fibrillar structure and further reduction in intra fibrillar diameter. Similar results were reported earlier by Oksman et al. (2006). Both CNW/S and CNW showed rod-like shapes with CNW presenting a smooth surface which may be due to partial solubilization of cellulose during esterification (Tang et al., 2013), while the CNW/S outline was slightly rough. After chemical swelling and acid hydrolysis, individual cellulose nanowhiskers were obtained. This result is further supported by TEM analysis, which will be discussed in detail in the next section.

### 4.3. Transmission electron microscopy

TEM is considered to be a powerful technique in the characterization of cellulose nanowhiskers (Maria, Garcia, & Lagaron, 2010). The effect of chemical swelling and acid hydrolysis treatments on MCC is shown in Fig. 3. Analysis of the suspension revealed

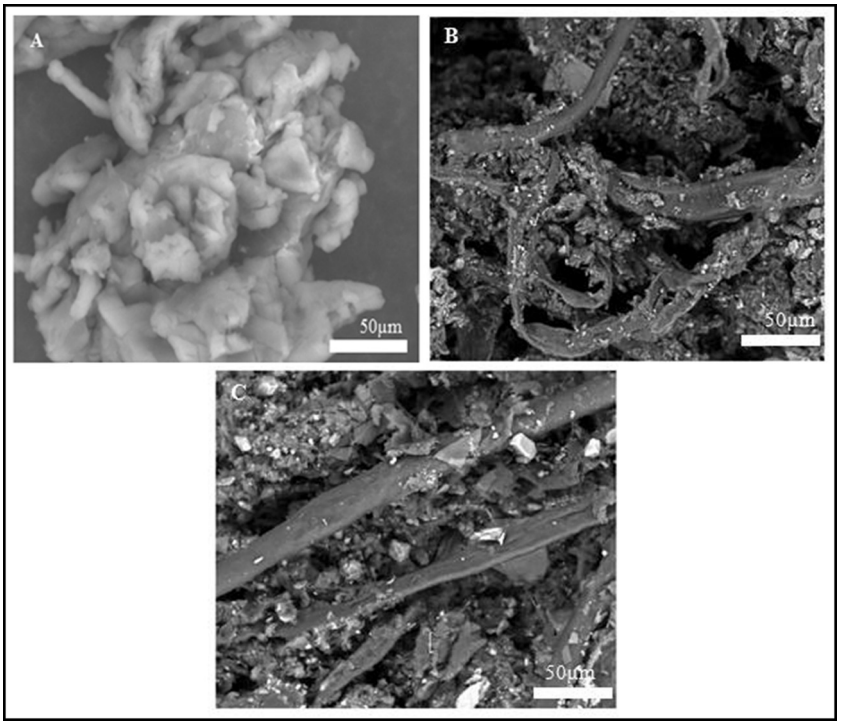


**Fig. 2.** Typical scanning electron micrographs of (A) MCC, (B) CNW/S, and (C) CNW.

remarkable changes in the morphological features of MCC (Fig. 3(A)) after treatment. It is clearly observed from TEM analysis that MCC has likely agglomerated to form large MCC particles in the micron range. However, after treatment, individual whiskers (crystals) were obtained showing a rod-like structure. The average size distribution of the whiskers from both treatments were analyzed and found to be in the nanometer range. Indeed the length of the CNW/S (Fig. 3(B)) and CNW (Fig. 3(C)) is estimated to be more than 100 nm while the diameter was estimated to be less than 10 nm for CNW and 20 nm for CNW/S.

It is interesting to note that the chemical swelling treatment displayed individual whiskers as compared to the aggregated structures obtained for acid hydrolysis. The apparent agglomeration of the whiskers was still present in the CNW (Fig. 3(C)) sample. It is not clear whether this was due to drying of the suspension (evaporation of water) onto the carbon film covering the copper grids

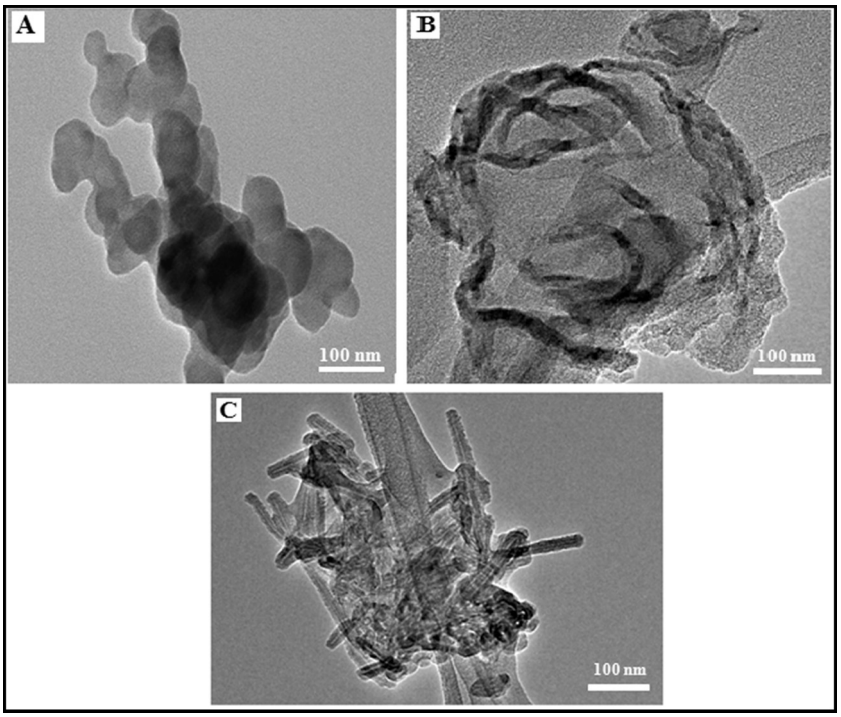


**Fig. 3.** Typical transmission electron micrographs for (A) MCC, (B) CNW/S and (C) CNW.

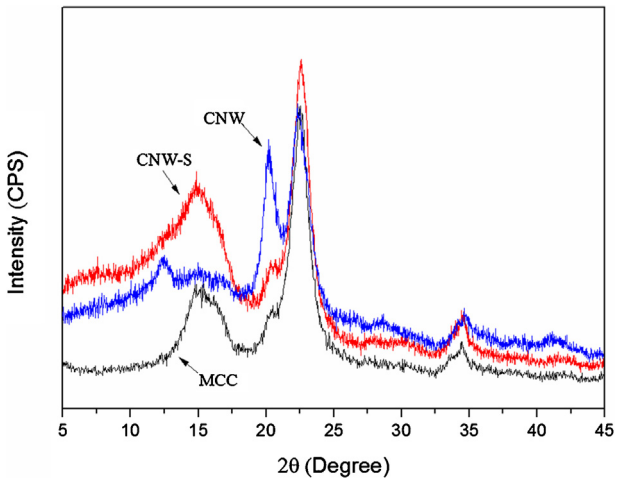


**Fig. 4.** X-ray diffractograms from MCC, CNW/S and CNW.

or the true state of the suspension. Similar observation was also reported in previous studies (Jonoobi et al., 2011; Kvien, Tanem, & Oksman, 2005; Wang, Ding, & Cheng, 2007). However, according to H. Liu et al. (2010) it is possible that this agglomeration may be due to the surface ionic charge (esterification) caused by strong acid treatment. Therefore these types of whiskers tend to stack into special micro-sized particles due to surface electrostatic attraction (D. Liu et al., 2010; H. Liu et al., 2010).

### 4.4. X-ray diffraction

X-ray diffraction (X-RD) patterns of natural lignocellulosic fibers are known to display a typical crystal lattice of cellulose type I, with the main diffraction signals at 2$\theta$ values of 15°, 16°, 22.5° and 34° (De Menezes et al., 2009). The X-RD spectra of MCC, CNW/S and CNW are shown in Fig. 4. The crystallinity values are tabulated in Table 2. The X-RD pattern was the same for MCC and CNW/S samples, being that of typical cellulose I with no cellulose II present. In essence, this indicates that the MCC structure was not significantly changed by the chemical swelling treatment and most of the crystalline regions are preserved. This point to the fact that the chemicals used did not spread beyond the crystalline part, and that swelling took place only between the crystalline areas (Jonoobi et al., 2011). Interestingly, as shown in Fig. 4 a new peak appeared at 21° for MCC after acid hydrolysis suggesting the coexistence of cellulose I and cellulose II allomorphs. A similar finding was reported by Mandal and Chakrabarty (2011) in the isolation of nanocellulose from waste sugarcane baggase.

From Table 2, it is obvious that the crystallinity value of the CNW/S is higher than MCC after treatment. On the other hand the crystallinity of CNW was slightly decreased compared to MCC and CNW/S due to the esterification of cellulose chains after acid hydrolysis ($H_2SO_4$). A decrease in crystallinity after acid hydrolysis was also observed by Tang et al. (2013) in a microstructural study of cellulose nanocrystal from pure wood pulp filter paper. In addition, according to Wang et al. (2007), this phenomenon was probably because the surface amorphous ratio of CNW was high

**Table 2**
Crystallinity of MCC, CNW/S, and CNW.

| Samples | Crystallinity (%) |
|---|---|
| MCC | 87 |
| CNW-S | 88 |
| CNW | 84 |

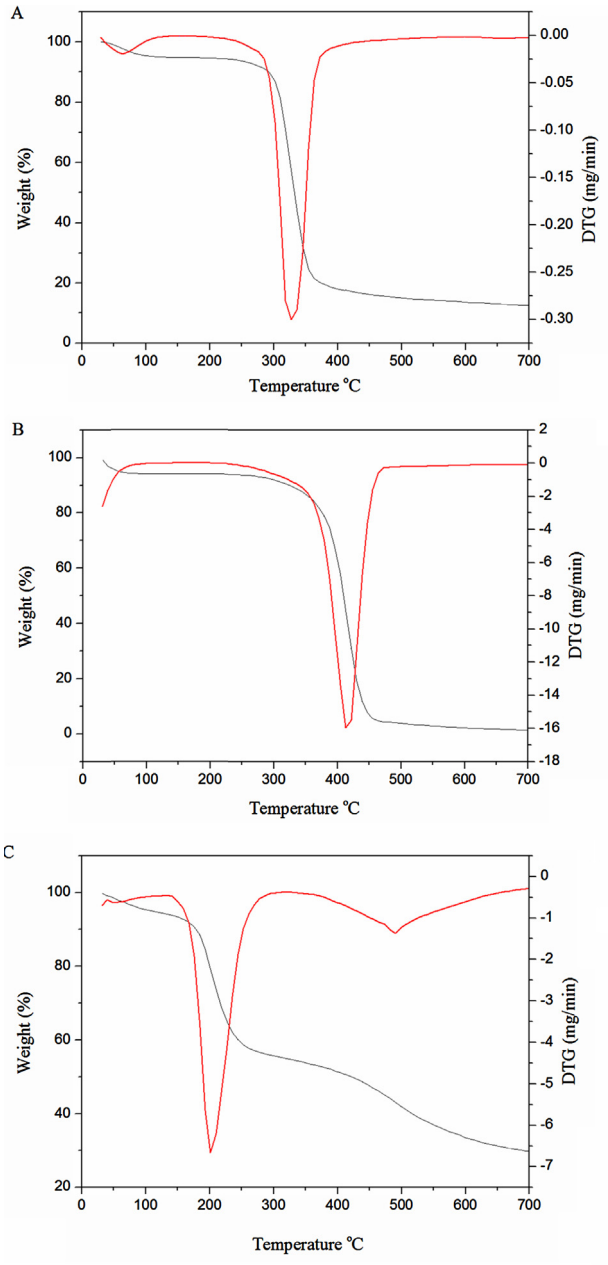


**Fig. 5.** Typical TGA and DTG curves for (A) MCC, (B) CNW/S and (C) CNW.

because of their high specific surface area, which leads to differences in thermal degradation behavior. This will be discussed in detail in the next section. However, from the X-RD results, it can be concluded that the cellulose nanowhiskers from MCC obtained by two different treatments (CNW/S and CNW) gives the higher crystallinity value as compared to those reported by Li et al. (2009) in the extraction of cellulose nanowhiskers from mulberry, which yielded a crystallinity of 73.4%.

### 4.5. Thermogravimetric analysis

The thermal stability of CNW/S and CNW after chemical swelling and acid hydrolysis were studied by thermogravimetric analysis (TGA) and derivative thermogram (DTG) as compared to that of MCC. The TGA and DTG curves for all samples are graphically represented in Fig. 5. The thermal degradation data ($T_{on}$), ($T_{10\%}$), ($T_{50\%}$),

**Table 3**
Thermal properties of MCC, CNW/S and CNW.

| Samples | Degradation temp. (°C) | | | DTG peak temp., $T_{max}$ | | Residual weight (%) at 700 °C |
|---|---|---|---|---|---|---|
| | $T_{on}$ | $T_{10}$ | $T_{50}$ | $T_{max\,1}$ | $T_{max\,2}$ | |
| MCC | 275 | 293 | 327 | 326 | – | 12.55 |
| CNW-S | 329 | 345 | 413 | 418 | – | 1.39 |
| CNW | 125 | 176 | 414 | 201 | 490 | 30.0 |

the residual weight at 700 °C as well as the peak degradation temperatures ($T_{max}$) are listed in Table 3.

The figure clearly reveals that chemical swelling and acid hydrolysis treatment changed the thermal stability of MCC (Fig. 5(A)). CNW/S (Fig. 5(B)) presented a higher degradation temperature ($T_{on}$, $T_{10\%}$ and $T_{50\%}$) when compared with the MCC. This demonstrates that CNW/S has better thermal stability compared to MCC. The higher decomposition temperature obtained was attributed to the greater crystallinity of cellulose material (Rosa et al., 2012). As indeed evidenced by X-RD diffraction study, the crystallinity of CNW/S was high and this was probably responsible for the thermal stability of CNW/S. As well, the rearrangement and reorientation of the crystals in cellulose raises the onset degradation temperature (Mandal & Chakrabarty, 2011).

However, CNW (Fig. 5(C)) showed significantly different degradation behavior than CNW/S and MCC. In the case of CNW, lower degradation onset ($T_{on}$ and $T_{10\%}$) was recorded, showing a two-step degradation process (Table 2) as revealed by the DTG curve, where the higher temperature stage ($T_{max\,2}$) may be related to the breakdown of the interior of unsulfured crystals similar to that reported by Li et al. (2009). The difference in thermal degradation behavior of CNW arose from the differences in outer surface structure of nano-crystalline particles including the presence of sulphate groups (Wang et al., 2007). According to Herrera, Mathew, and Oksman (2012), during acid hydrolysed MCC with $H_2SO_4$, sulphate groups will be introduced into the whiskers surface. These sulphate groups probably affected the thermal stability of the whiskers due to dehydration reaction. It is also believed that cellulose hydrolysis not only dissolves the amorphous regions, but also some crystalline regions making them more susceptible to degradation at elevated temperatures (Bras et al., 2010; Mandal & Chakrabarty, 2011).

It is interesting to note that the CNW shows highest residues at 700 °C as compared to CNW/S and MCC. CNW has the highest weight residue because of sulphate groups which act as a flame retardant, ostensibly serving as a protective barrier to both mass and energy from the burning surface to the attached polymeric chains (Li et al., 2009). In view of the above results, it was concluded that the CNW/S and CNW from MCC sample produced by two different treatments have better thermal stability than MCC and will be suitable for use as reinforcements in the production of green bio-composites.

## 5. Conclusion

Cellulose nanowhiskers from oil palm biomass MCC were prepared by chemical swelling treatment and acid hydrolysis. The cellulose surface remains unaltered after treatment as revealed by FT-IR analysis. Both treatments changed the morphology of MCC, where the agglomeration was broken down to individual whiskers. The obtained nano-scaled whiskers from swelling treatment showed typical cellulose I structure. However, acid hydrolysis showed the coexistence of cellulose II structure. It can be concluded from these results that the produced cellulose nanowhiskers exhibited better thermal properties than MCC, making them suitable as reinforcing agents in bio-renewable composite preparation.

## Acknowledgements

The author M.K. Mohamad Haafiz would like to thank University Sains Malaysia (USM), Ministry of Higher Education Malaysia (KPT) and Research University Grant 05H22 sub-code Q.J130000.2509.05H22 for the financial support.

## References

Bondeson, D., Mathew, A., & Oksman, K. (2006). Optimization of the isolation of nanocrystals from microcrystalline cellulose by acid hydrolysis. *Cellulose*, *13*(2), 171–180.

Bras, J., Hassan, M. L., Bruzesse, C., Hassan, E. A., El-Wakil, N. A., & Dufresne, A. (2010). Mechanical, barrier, and biodegradability properties of bagasse cellulose whiskers reinforced natural rubber nanocomposites. *Industrial Crops and Products*, *32*, 627–633.

Brito, B. S. L., Pereira, F. V., Putaux, J. L., & Jean, B. (2012). Preparation, morphology and structure of cellulose nanocrystals from bamboo fibers. *Cellulose*, *19*, 1527–1536.

Chen, Y., Liu, C., Chang, P. R., Cao, X., & Anderson, D. P. (2009). Bionanocomposites based on pea starch and cellulose nanowhiskers hydrolyzed from pea hull fibre: Effect of hydrolysis time. *Carbohydrate Polymers*, *76*, 607–615.

Cherian, B. M., Leão, A. L., de Souza, S. F., Costa, L. M. M., de Olyveira, G. M., Kottaisamy, M., et al. (2011). Cellulose nanocomposites with nanofibres isolated from pineapple leaf fibers for medical applications. *Carbohydrate Polymers*, *86*, 1790–1798.

De Menezes, A. J., Siqueira, G., Curvelo, A. A. S., & Dufresne, A. (2009). Extrusion and characterization of functionalized cellulose whiskers reinforced polyethylene nanocomposites. *Polymer*, *50*, 4552–4563.

Deepa, B., Abraham, E., Cherian, B. M., Bismarck, A., Blaker, J. J., Pothan, L. A., et al. (2011). Structure, morphology and thermal characteristics of banana nanofibers obtained by steam explosion. *Bioresource Technology*, *102*, 1988–1997.

Eichhorn, S. J. (2010). Cellulose nanowhiskers: Promising materials for advanced applications. *Soft Matter*, *7*, 303–315.

Fahma, F., Iwamoto, S., Hori, N., Iwata, T., & Takemura, A. (2010). Isolation, preparation, and characterization of nanofibers from oil palm empty-fruit-bunch (OPEFB). *Cellulose*, *17*, 977–985.

Fernandes, A. N., Thomas, L. H., Altaner, C. M., Callow, P., Forsyth, V. T., Apperley, D. C., et al. (2011). Nanostructure of cellulose microfibrils in spruce wood. *Proceedings of the National Academy of Sciences of the United States of America*, *108*, 1195–1203.

Filson, P. B., & Dawson-Andoh, B. E. (2009). Sono-chemical preparation of cellulose nanocrystals from lignocelluloses derived materials. *Bioresource Technology*, *100*, 2259–2264.

Haafiz, M. K. M., Eichhorn, S. J., Hassan, A., & Jawaid, M. (2013). Isolation and characterization of microcrystalline cellulose from oil palm biomass residue. *Carbohydrate Polymers*, *93*, 628–634.

Hassan, A., Salema, A. A., Ani, F. N., & Bakar, A. A. (2010). A review on oil palm empty fruit bunch fiber-reinforced polymer composite materials. *Polymer Composites*, *31*, 2079–2101.

Herrera, M. A., Mathew, A. P., & Oksman, K. (2012). Comparison of cellulose nanowhiskers extracted from industrial bio-residue and commercial microcrystalline cellulose. *Materials Letters*, *71*, 28–31.

Jain, P., & Vigneshwaran, N. (2012). Effect of Fenton's pretreatment on cotton cellulosic substrates to enhance its enzymatic hydrolysis response. *Bioresource Technology*, *103*, 219–226.

Johar, N., Ahmad, I., & Dufresne, A. (2012). Extraction, preparation and characterization of cellulose fibres and nanocrystals from rice husk. *Industrial Crops and Products*, *37*, 93–99.

Jonoobi, M., Khazaeian, A., Md.Tahir, P., Azry, S. S., & Oksman, K. (2011). Characteristics of cellulose nanofibers isolated from rubberwood and empty fruit bunches of oil palm using chemo-mechanical process. *Cellulose*, *18*, 1085–1095.

Kumar, V., Maria De La, L. R. M., & Yang, D. (2002). Preparation, characterization, and tabletting properties of a new cellulose-based pharmaceutical aid. *International Journal of Pharmaceutics*, *235*, 129–140.

Kvien, I., Tanem, S., & Oksman, K. (2005). Characterization of cellulose whiskers and their nanocomposites by atomic force and electron microscopy. *Biomacromolecules*, *6*(6), 3160–3165.

Lee, S. Y., Mohan, D. J., Kang, I. A., Doh, G. H., Lee, S., & Han, S. O. (2009). Nanocellulose reinforced PVA composite films: Effects of acid treatment and filler loading. *Fibers and Polymers*, *10*, 77–82.

Li, R., Fei, J., Cai, Y., Li, Y., Feng, J., & Yao, J. (2009). Cellulose whiskers extracted from mulberry: A novel biomass production. *Carbohydrate Polymers*, *76*, 94–99.

Liu, D., Zhong, T., Chang, P. R., Li, K., & Wu, Q. (2010). Starch composites reinforced by bamboo cellulosic crystals. *Bioresource Technology*, *101*, 2529–2536.

Liu, H., Liu, D., Yao, F., & Wu, Q. (2010). Fabrication and properties of transparent polymethylmethacrylate/cellulose nanocrystals composites. *Bioresource Technology*, *101*, 5685–5692.

Mandal, A., & Chakrabarty, D. (2011). Isolation of nanocellulose from waste sugarcane bagasse (SCB) and its characterization. *Carbohydrate Polymers*, *86*, 1291–1299.

Maria, D., Garcia, S., & Lagaron, J. M. (2010). On the use of plant cellulose nanowhiskers to enhance the barrier properties of polylactic acid. *Cellulose*, *17*, 987–1004.

Mathew, A. P., Oksman, K., & Sain, M. (2005). Mechanical properties of biodegradable composites from poly lactic acid (PLA) and microcrystalline cellulose (MCC). *Journal of Applied Polymer Science*, *97*, 2014–2025.

Mathew, A. P., Oksman, K., & Sain, M. (2006). The effect of morphology and chemical characteristics of cellulose reinforcements on the crystallinity of polylactic acid. *Journal of Applied Polymer Science*, *101*, 300–310.

Nishiyama, Y. (2009). Structure and properties of the cellulose microfibril. *Journal of Wood Science*, *55*, 241–249.

Oksman, K., Mathew, A. P., Bondeson, D., & Kvien, I. (2006). Manufacturing process of cellulose whiskers/polylactic acid nanocomposites. *Composites Science and Technology*, *66*, 2776–2784.

Pandey, J. K., Chu, W. S., Kim, C. S., Lee, C. S., & Ahn, S. H. M. (2009). Bio-nano reinforcement of environmentally degradable polymer matrix by cellulose whiskers from grass. *Composites: Part B*, *40*, 676–680.

Pereda, M., Amica, G., Rácz, I., & Marcovich, N. E. (2011). Structure and properties of nanocomposite films based on sodium caseinate and nanocellulose fibers. *Journal of Food Engineering*, *103*, 76–83.

Petersson, L., Kvien, I., & Oksman, K. (2007). Structure and thermal properties of poly(lactic acid)/cellulose whiskers nanocomposite materials. *Composites Science and Technology*, *67*, 2535–2544.

Rånby, B. G. (1951). Cellulose and muscle – The colloidal properties of cellulose micelles. *Discussions of the Faraday Society*, *11*, 158–164 (discussion 208–213).

Rosa, S. M. L., Rehman, N., De Miranda, M. I. G., Nachtigall, S. M. B., & Bica, C. I. D. (2012). Chlorine-free extraction of cellulose from rice husk and whisker isolation. *Carbohydrate Polymers*, *87*, 1131–1138.

Samir, M. A. S. S., Alloin, F., & Dufresne, A. (2005). Review of recent research into cellulosic whiskers, their properties and their application in nanocomposite field. *Biomacromolecules*, *6*, 612–626.

Shinoj, S., Visvanathan, R., Panigrahi, S., & Kochubabu, M. (2011). Oil palm fiber (OPF) and its composites: A review. *Industrial Crops and Products*, *33*, 7–22.

Tang, L., Huang, B., Lu, Q., Wang, S., Ou, W., Lin, W., et al. (2013). Ultrasonication-assisted manufacture of cellulose nanocrystals esterified with acetic acid. *Bioresource Technology*, *127*, 100–105.

Wang, N., Ding, E., & Cheng, R. (2007). Thermal degradation behaviors of spherical cellulose nanocrystals with sulfate groups. *Polymer*, *48*.

Yano, H., Sugiyama, J., Nakagaito, A. N., Nogi, M., Matsuura, T., Hikita, M., et al. (2005). Optically transparent composites reinforced with networks of bacterial nanofibers. *Advanced Materials*, *17*, 153–155.